Gynecologic Oncology 152 (2019) 387–395

Contents lists available at ScienceDirect

Gynecologic Oncology

journal homepage: www.elsevier.com/locate/ygyno

NCK1 promotes the angiogenesis of cervical squamous carcinoma via Rac1/PAK1/MMP2 signal pathway

Xia Pei [a], Huang Mingchuan [b], Zhang Yuting [a], Xiong Xiujuan [a], Yan Min [a], Xiong Xiaoliang [a], Yu Weiwei [a], Song Enlin [a,*]

[a] Department of Pathology, Basic Medical College of Nanchang University, Nanchang, Bayi Road, 330006, China
[b] Department of Urology, the First Affiliated Hospital of Nanchang University, Nanchang, Yong Wai zheng Road, 330006, China

HIGHLIGHTS

- Nck1 is overexpressed in cervical squamous cell carcinoma and associated with the cancer angiogenesis.
- Nck1 promotes the angiogenesis-inducing capacity of cervical cancer cells via up-regulation of MMP2.
- Nck1 activates the Rac1/PAK1 signaling to up-regulate MMP2 expression of cervical cancer cells.
- Inhibition of Rac1/PAK1 signaling impaired the pro-angiogenic role of Nck1 in cervical squamous carcinoma.

GRAPHICAL ABSTRACT

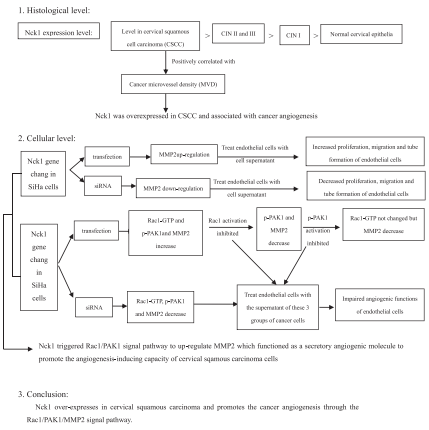

ARTICLE INFO

Article history:
Received 17 September 2018
Received in revised form 4 November 2018
Accepted 9 November 2018
Available online 13 November 2018

Keywords:
Nck1
Angiogenesis
MMP2
Rac1
PAK1
CSCC

ABSTRACT

Objective. The study was to explore the roles of Nck1 in the angiogenesis of cervical squamous cell carcinoma (CSCC).

Methods. mRNA and protein levels were evaluated with real-time quantitative PCR and immunohistochemisty/western blotting respectively. The cancer microvessel density (MVD) was assayed with CD34 endothelial labeling. Nck1 gene knock-in (SiHa-Nck1+) and knock-down (SiHa-Nck1-) were achieved by gene transfection and siRNA respectively. Protein level from cellular supernatant was measured with ELISA. Proliferation, migration and tube formation of the Human Umbilical Vein Endothelial cells (HUVECs) were evaluated by CCK-8 cell viability assay, transwell chamber assay and in vitro Matrigel tubulation assay respectively.

Results. Nck1 level gradually increased from normal cervical epithelia to high-grade CIN, overexpressed in CSCC and was associated with cancer MVD. The ability of proliferation, migration and tube formation of HUVECs was enhanced in SiHa-Nck1+-treated while decreased in SiHa-NcK1−-treated cells compared to SiHa-control-treated cells. Mechanistically, RAC1-GTP, p-PAK1 and MMP2 were increased in SiHa-NCK1+ cells and pretreatment with the Rac1 inhibitor (NSC23766) significantly decreased their levels. Furthermore, inhibition of PAK1 reduced MMP2 level in SiHa-Nck1+ cells whereas the level of Rac1-GTP was unaltered. Also, inhibition of Rac1 or PAK1 impaired angiogenesis-inducing capacity of cancer cells.

* Corresponding author at: Department of Pathology, Basic Medical College of Nanchang University, Nanchang, Bayi Road, 330006, China.
E-mail address: songenling@126.com (E. Song).

https://doi.org/10.1016/j.ygyno.2018.11.013

Conclusions. Nck1 promotes the angiogenesis-inducing capacity of CSCC via the Rac1/PAK1/MMP2 signal pathway.

1. Introduction

Angiogenesis is one of the key mechanisms responsible for growth, invasion and metastasis of solid carcinoma [1]. It not only provides the blood supply [2] for cancer cells but also promotes the metastasis of cancer cells into the blood vessels due to the high permeability of the new microvessels. In addition, angiogenesis in itself is tissue invasive by the process of endothelial sprouting [3], which facilitates the cancer cells to spread locally. Accumulating evidence suggests that a variety of pro-angiogenetic factors are associated with cancer progression, including cancer invasion [4], lymph node metastasis [5], clinical stages [6] and drug resistance [7]. Angiogenesis has been demonstrated to correlate with poor prognosis of cervical cancer [8,9] and some angiogenic molecules are suggested as therapeutic targets [10]. A novel VEGF receptor-2 kinase inhibitor, apatinib, has shown to have anti-cancer effect for a variety of solid tumors [11,12]. Especially, Bevacizumab (a fully humanized anti-VEGF antibody) in combination with other drugs constitute first-line therapy for recurrent/metastatic cervical carcinoma, which improves the overall survival of the patients [13]. However, some cancers are resistant to Bevacizumab [7,14 and 15] such as advanced gynecologic cancers [16]. Therefore, identification of novel angiogenic molecules is significant for targeting cervical cancer.

Nck1, originally found in human melanoma cells, is an intracellular signal adaptor protein with Src homology 2 and 3 (SH2 and SH3) domains [17]. Nck1 binds to many tyrosine kinase receptors [18] or phosphotyrosine docking proteins through SH2 domain and then recruits downstream small G proteins or proline-rich sequences-containing effecter proteins through the SH3 domain [19], thus transmitting receptor tyrosine kinase signaling to regulate multiple biological processes such as cytoskeletal rearrangement, cell proliferation [20] and migration [21]. Nck1 may function as an oncogene in cancer development as several studies have revealed that Nck1 can promote the proliferation and infiltration [22] of liver cancer [19] and breast cancer [23].

As a signal adapter protein, Nck1 has been demonstrated to be able to activate Rac1, a member of the Rho subfamily of small G protein [24]. Rac1 activation has been shown to regulate angiogenesis through the Rac1-PAK1 signaling [25], implying Nck1 may play important roles in cancer angiogenesis. Intriguingly, Nck1 has been recently found to be differentially expressed between cervical cancer tissue and normal cervical epithelial tissue [26], indicating Nck1 may also be involved in the development and progression of cervical cancer. However, the specific biological function of Nck1 in cervical carcinoma remains unclear. The present study was designed to investigate the association between Nck1 and the angiogenesis of CSCC.

2. Materials and methods

2.1. Patients' samples

Specimens used were collected from the Department of Pathology, First Affiliated Hospital of Sun Yat-sen University, China and were approved by The Institutional Research Board of Universtiy, Jiangxi Medical Center. 40 cases of pre-invasive specimens and 50 cases of invasive specimens from the CSCC patients without radiotherapy and chemotherapy before surgery were used in this study. The pre-invasive specimens included 10 cases of CIN I (Cervical Intraepithelial Neoplasia), 15 of CIN II and 15 of CIN III (including 5 cases of carcinoma in situ). All the specimens were formalin-fixed and paraffin-embedded, and the histological diagnosis for all the cases was further confirmed by two clinical pathologists with hematoxylin and eosin staining. The mean patient age was 49.7 ± 11.68 (ranging from 33 to 75). Nineteen tumors had parametrial involvement. Lymph node metastasis was present in 25 cases and vascular invasion was found in 26 cases. Fourteen tumors were ≥ 4 cm in its diameter. Sixteen tumors were of poor differentiation and 34 tumors were of moderate to high differentiation. According to the FIGO (International Federation of Gynecology and Obstetrics) staging, 18 cases belong to FIGO I (7 IA and 11 IB), 11 cases belong to FIGO IIA and 21 cases belong to FIGO IIB. In addition, another 17 cases of normal cervical squamous epithelium were selected as control.

2.2. Immunohistochemistry

Immunohistocchemistry were conducted as previously described [27]. Briefly, after antigen retrieval, dewaxed and rehydrated, sections were treated with 3% hydrogen peroxide and then 5% bovine serum albumin. After incubation overnight at 4 °C with primary antibody (rabbit polyclonal anti-Nck1 antibody[Y531], ab32120; abcam), slides were then incubated with MaxVision™ HRPPolymer IgG complexes (KIT5150; Maixin-Bio, Shenzhen, China) for 30 min. Then, sections were incubated with DAB (DAB-0031; Maixin-Bio, Shenzhen, China) for 1–5 min. The histology was quantified with Image Pro Plus 6.0 to detect the photodensity. Each slide was counted 5 fields and average of integral optical density (IOD) was indicated as intensity of protein expression.

2.3. Microvessel density assessment

Microvessel density (MVD) assessment was performed as previously described [27]. After endothelial labeling by endothelial CD34 (mouse monoclonal, anti-CD34, KIT-0004; Maixin-Bio) the microvessels were counted. Single endothelial cells, cell clusters, microvessels separated from adjacent microvessels and branching structures were all counted as a single vessel. Peritumoral vessels, vascularity in necrosis, sclerotization, and the vessels with thick smooth muscle or in a diameter larger than 8 erythrocytes were not counted. All counts were performed in a blind fashion.

2.4. Cell culture and treatment

The human cervical squamous carcinoma cell line SiHa (TCHu113, cell bank of Chinese Academy of Sciences, Shanghai, China) was routinely cultured in Dulbecco modified Eagle medium supplemented with 10% (vol/vol) fetal bovine serum (FBS), 100 IU/mL penicillin G plus 100 μg/mL streptomycin sulfate. The human umbilical vein endothelial cells (HUVECs; FH0287; FuHeng Biology, Shanghai, China) were also cultured with endothelial cell growth medium. Nck1 gene transfection and siRNA were performed according to manufacturer's instruction. For Nck1 gene transfection (SiHa-Nck1+), 1 μg of pCMV2-Nck1 (Maijie, Nantong, China) and 3 μL of liposome SuperFectinTM II (Pufei Biotech, Shanghai, China) in 50 μL of serum-free high-sugar medium were mixed gently to form a transfection complex. For Nck1 gene knockdown (SiHa-Nck1-), 1 μg siRNA-Nck1(5′-GGCCTTCACTCACTGG AAA-3′) (PPL, Nanjing, China) and 3 μL of liposome SuperFectinTM II (Pufei Biotech, Shanghai, China) in 50 μL of serum-free medium were mixed to form a RNAi complex. Both mixture were incubated for 5 min and laid for 25 min at room temperature and then were added to cells. The SiHa cells transfected with empty plasmid vector (SiHa-

vec) or scrambled siRNA (SiHa-src) were used as a negative control of gene transfection and Nck1 siRNA, respectively, and the untransfected cells were used as a blank control.

2.5. RNA extraction and real-time (RT) quantitative polymerase chain reaction (qPCR)

The qPCR was performed according to the kit (SYBR® Green Master Mix in an ABI PRISM® 7500 Sequence Detection System, Applied Biosystems Inc., Foster City, CA, United States). After total RNA extraction and cDNA synthesis (primer: NCK1, 5′-TCTAAGTCCTGGTGGCGAG TTCG-3′,5′-CAGGAGATGCAGAATCTGGCACAC-3′; MMP2, 5′-ATGCAG TGGGGG. CTTAAGAA-3′, 5′-GGTATTGCATGTGCTAGGTAAGC-3′; β-actin, 5′-CCTGGCACCCAGCAC. AAT-3′, 5′-GGGCCGGACTCGTCATAC-3′). qPCR thermal cycling were: 94 °C for 30 s, 40 cycles of amplifications at 94 °C for 5 s and then 60 °C for 30 s. Amplification specificity was determined using a melting curve, and results were processed by software provided with an ABI7500 PCR instrument. Gene expression was quantified using the ΔΔCT calculation with CT as the threshold cycle. The relative levels of target genes, normalized to the sample with the lowest CT, were given as $2^{-\Delta\Delta CT}$ [28]. The β-actin was used as an internal control.

2.6. Western blotting

Briefly, after cell lysate preparation and protein content quantification, the lysate was loaded into SDS-PAGE for separation and then was transferred to nitrocellulose filter membrane. Probed with corresponding primary antibodies (rabbit molyclonal anti-Nck1, ab32120, abcam, USA; rabbit polyclonal anti-MMP2, 10,373-2-AP, ProteinTech, USA; rabbit polyclonal anti-PAK1, 21,401-1-AP, ProteinTech; rabbit polyclonal anti- Phospho-PAK1(Thr423), AF4463, Affinity, USA and Active Rac1 pull-Down and Detection kit, 16,118, Thermo Fisher scientific, USA), the membrane was incubated with a horseradish peroxidase–conjugated secondary goat antirabbit IgG. The signal was detected using chemiluminescence EasySee Western Blot kit (Jiangsu KeyGEN BioTECH Corp., Ltd). β-actin was used as an internal control.

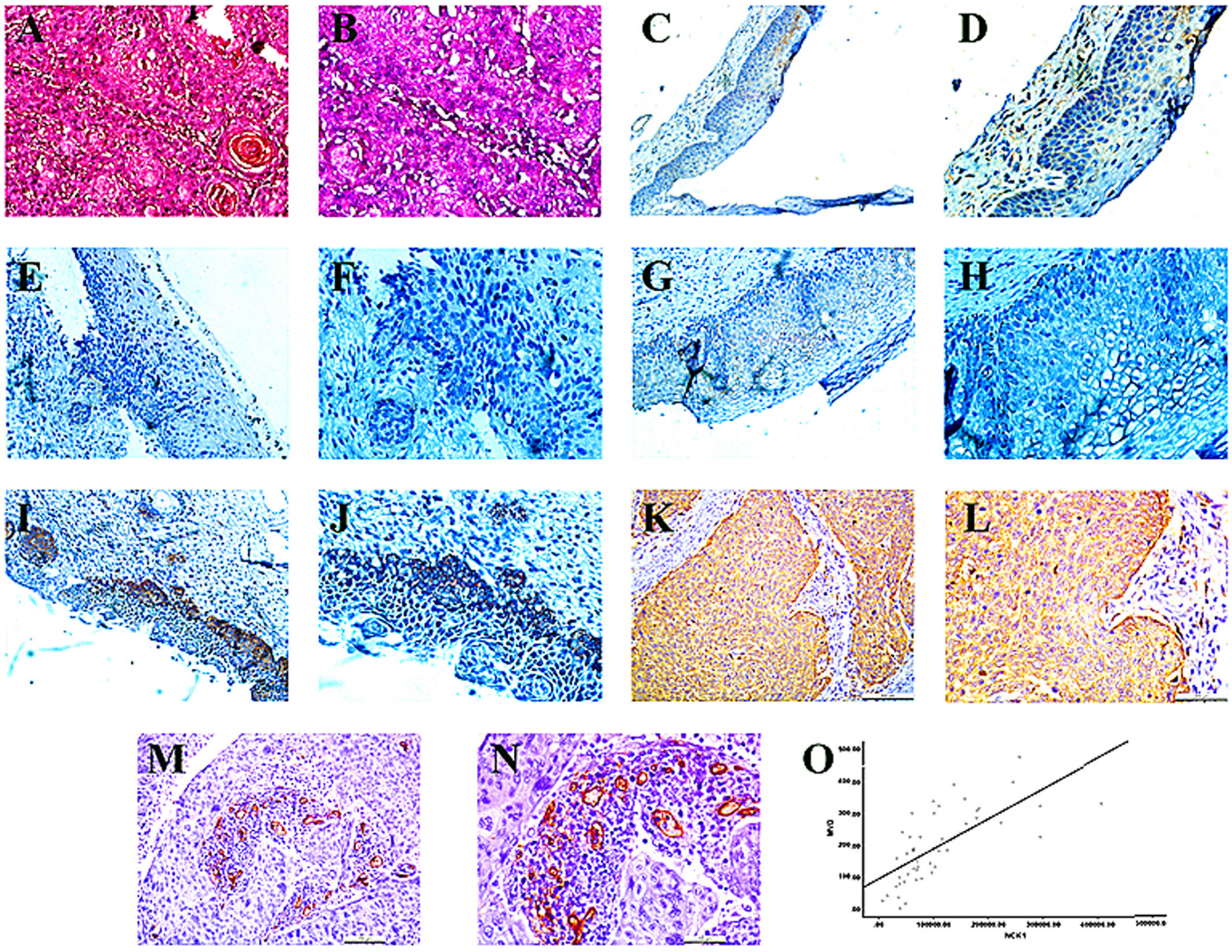

Fig. 1. Nck1 expression in normal cervical epithelia, CIN and CSCC tissues and its correlation with cancer MVD. **A**, Hematoxylin and eosin staining of CSCC samples (original magnification ×200). **B**, Hematoxylin and eosin staining of CSCC samples (×400). **C**, Expression of Nck1 in normal cervical squamous epithelium (×100). **D**, Expression of Nck1 in normal cervical squamous epithelium (×200). **E**, Expression of Nck1 in CIN I (×200). **F**, Expression of Nck1 in CIN I (×400). **G**, Expression of Nck1 in CIN II (×200). **H**, Expression of Nck1 in CIN II (×400). **I**, Expression of Nck1 in CIN III (×200). **J**, Expression of Nck1 in CIN III (× 400). **K**. Expression of Nck1 in CSCC tissue (×200). **L**, Expression of Nck1 in CSCC tissue (×400). **M**, Microvessels labeled by endothelial CD34 in CSCC tissue (×200). **N**, Microvessels labeled by endothelial CD34 in CSCC tissue (×400). **O**, Expression level of Nck1 was positively correlated with the MVD of CSCC, $r = 0.7$, $p < 0.001$.

2.7. MMP2 enzyme linked-immuno-sorbent assay

The ELISA was performed according to a Human MMP2 ELISA Kit (KE00077, ProteinTech, USA) instruction. After adding the supernatant of target cells (2×10^5/mL × 500 μL) and gradient concentration of standard protein, the ELISA plates were incubated at 37 °C for 90 min and then biotinylated MMP2 antibody was added and incubated at 37 °C for 60 min. Followed with Streptavidin-HRP addition and incubation for 30 min, tetramethyl-benzidine (TMB) reagent was added to develop the signals at 37 °C in dark for 8 to 14 min. The signals were detected at A450 nm on an ELISA reader. MMP2 protein was quantified using the regression equation formula. All experiments were repeated 3 times.

2.8. Cell proliferation assay

Cell Counting Kit-8(ZP328-2, BeiJing zoman Biotechnology Co. Ltd) was used to measure the HUVEC proliferative activity. Briefly, 3×10^3 cells were plated into 96-well plates. After the indicated time of culture, CCK-8 reagent was added and absorbance was measured at 450 nm. Each experiment was done in sextuplicate.

2.9. Cell migration assay

Migratory ability of HUVECs was assessed using a Transwell Permeable Supports System (353,097; BD Company, Franklin Lakes, NJ). Briefly, 1×10^4 cells in 100 μL serum-free medium were seeded in the upper wells of the Transwell chambers, over which a thin layer of extracellular Matrigel was dried. The DMEM (600 μL) containing 20% FBS was added as a chemoattractant into the lower well of the chamber. After 24 h of incubation at 37 °C, the migrated cells contained in the membranes were fixed and subsequently stained with Crystal Violet stain. The membranes were mounted on glass slides, and migrated cells were counted at ×100 magnification. Each culture condition was conducted in triplicate.

2.10. Endothelial tube formation assay

Matrigel Matrix (ECM625, merck Millipore, USA) was diluted with serum-free endothelial cell growth medium to the ratio of 1:1 and then was added to a prechilled 96-well plate (50 μL) to allow to solidify for 1 h at 37 °C. Cells (1×10^5) suspended in 100 μL growth medium containing 5% FBS were seeded on the solidified Matrigel. After 2 h of routine culture different treatments were added into the desired wells. With further culture for 10 h, the cells were fixed with 4% paraformaldehyde. Then every tube with connected wall of endothelial bundles was counted as one tube under medium magnification (×20). The mean value of the 3 areas represents the tube-formation capacity of the endothelial cells.

2.11. Statistical analysis

Data were analyzed with SPSS19 (SPSS, Chicago, IL) and presented as mean ± SE. Student *t*-test was applied to compare the mean between groups. Correlation between Nck1 expression and cancer MVD was analyzed with Spearman correlation test.

3. Results

3.1. Nck1 was overexpressed in CSCC and associated with cancer angiogenesis

The diagnosis of CSCC was confirmed by hematoxylin and eosin staining (Fig. 1A–B). The carcinoma cells were obviously atypical with a netlike distribution and keratinization, suggesting an invasive CSCC. Both normal cervical squamous epithelium (Fig. 1C–D) and CIN I (Fig. 1E–F) showed weak expression of Nck1 in the basal/prickle cells respectively, with an IOD of 16,915.88 ± 4457.25 vs 19,024.23 ± 6226.38. In CIN II and CIN III (Fig. 1G–J), Nck1 was moderately expressed in almost whole layers of epithelium and the mean expression level (43,443.58 ± 5476.57) was significantly higher than that of normal epithelium ($p < 0.01$) and CIN I ($p < 0.01$). Importantly, cytoplastic and/or membranous expression of Nck1 in the tumor cells (Fig. 1K–L) (76,290.40 ± 1626.37) was significantly higher than that of CIN III ($p < 0.01$). These results suggested that Nck1 expression was gradually increased from normal cervical squamous epithelia to low-grade CIN and high-grade CIN and there was an overexpression of Nck1 in CSCC. The representative cancer microvessels labeled by endothelial CD34 was shown in Fig. 1M–N, and the mean MVD was 196.32 ± 113.07. Moreover, the Nck1 expression level was found to be positively correlated with the MVD of CSCC ($r = 0.7$, $p < 0.001$; Fig. 1O). The relationship between Nck1 expression and the clinicopathological parameters of CSCC was summarized in Table 1. Nck1 expression was related with the parametrial involvement ($p = 0.009$), lymph node metastasis ($p = 0.003$), vascular invasion ($p = 0.013$) and clinical stage ($p = 0.004$) of CSCC but not with the patients' age, differentiation degree and tumor size. These results suggest overexpression of Nck1 may be associated with the angiogenesis and progression of CSCC.

3.2. Nck1 promoted the angiogenesis-inducing capacity of SiHa cells

To further investigate the association between Nck1 and angiogenesis of CSCC, Nck1 gene was manipulated by gene transfection with pCMV2-Nck1 (SiHa-Nck1+) or siRNA-Nck1 (SiHa-Nck1-) in SiHa cells. Nck1 mRNA and protein levels were increased in SiHa-Nck1+ (439.45 ± 129.16, $p < 0.05$; 6.03 ± 0.20, $p < 0.05$, Fig. 2A–B) but decreased in SiHa-Nck1− (0.7584 ± 0.16555, $p < 0.05$; 0.337 ± 0.058, $p < 0.05$, Fig. 2C–D), compared to control SiHa cells. These results confirmed the success of knock-in and knock-down of Nck1 in SiHa cells. Then, the supernatants from SiHa, SiHa-Nck1+ and SiHa-Nck1− were used to stimulate the HUVECs (H-SiHa-Nck1+, H-SiHa-Nck1− and H-SiHa-con) to observe their angiogenic functions. As expected, the proliferation (Fig. 2E), migration (Fig. 2F–I) and tabulation (Fig. 2J–M) capacity were enhanced in H-SiHa-Nck1+ (127.24% ± 22.03%, $p < 0.05$; 266

Table 1
Relationship between Nck1 expression and clinicopathologic parameters of CSCC.

parameters	n	Nck1 expression	*p* Value
Age			0.190
<50	29	98,474.8 ± 79,006.83	
≥50	21	124,640.0 ± 67,170.45	
Differentiation			0.087
Moderate to high	34	119,884.0 ± 82,178.86	
Poor	16	87,322.0 ± 48,616.97	
Tumor size			0.141
<4 cm	36	118,103.3 ± 78,448.91	
≥4 cm	14	87,249.4 ± 58,741.62	
Clinical stage			0.004[a]
FIGO I and II A	29	83,142.8 ± 58,790.32	
FIGO II B	21	145,812.8 ± 79,132.00	
Parametrial involvement			0.009[b]
Absent	31	86,225.9 ± 57,786.73	
Present	19	147,379.2 ± 83,539.16	
Lymph node metastasis			0.003[c]
Absent	25	79,048.0 ± 56,997.08	
Present	25	139,880.3 ± 77,895.85	
Vascular invasion			0.013[d]
Absent	24	82,820.6 ± 64,636.57	
Present	26	134,058.2 ± 75,098.96	

[a] Nck1 level in the CSCC of FIGO II B stage was significantly higher than its level in the CSCC of FIGO I and II A stag, $p = 0.004$.
[b] Nck1 level in the CSCC with parametrial involvement was significantly higher than its level in the CSCC without parametrial involvement, $p = 0.009$.
[c] Nck1 level in the CSCC with lymph node metastasis was significantly higher than its level in the CSCC without lymph node metastasis, $p = 0.003$.
[d] Nck1 level in the CSCC with vascular invasion was significantly higher than its level in the CSCC without vascular invasion, $p = 0.013$.

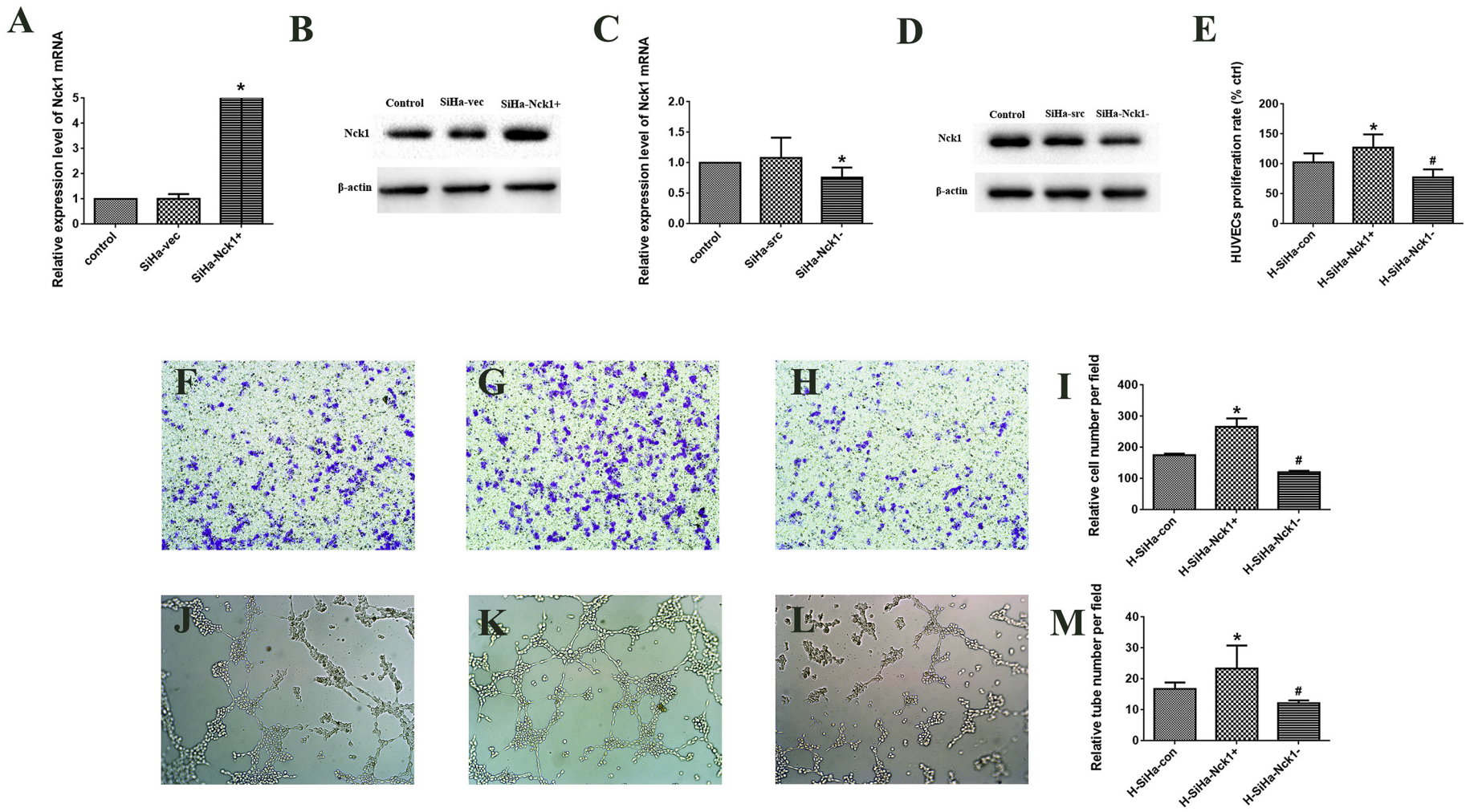

Fig. 2. Proliferation, migration and tube formation of the HUVECs stimulated with the supernatant from the SiHa cells with different Nck1 levels. **A**, Nck1 mRNA level of the SiHa cells transfected with pCMV2-Nck1 (**SiHa-Nck1+**) was significantly higher than that of normal SiHa cells (**con**) and the SiHa cells transfected with empty plasmid vector (**SiHa-vec**), *, **SiHa-Nck1+** vs **con** or **SiHa-vec**, $p < 0.001$. **B**, Nck1 protein level of **SiHa-Nck1+** was significantly higher than that of **con** and **SiHa-vec**, **SiH a-Nck1+** vs **con** or **SiHa-vec**, $p < 0.001$. **C**,Nck1 mRNA level of the SiHa cells transfected with Nck1 siRNA (**SiHa-Nck1−**) was significantly lower than that of normal SiHa cells (**con**) and the SiHa cells transfected with scrambled siRNA (**SiHa-src**), *, **SiHa-Nck1−** vs **con** or **SiHa-src**, $p < 0.05$. **D**, Nck1 protein level of **SiHa-Nck1−** was significantly lower than that of **con** and **SiHa-src**, **SiHa-Nck1−** vs **con** or **SiHa-src**, $p < 0.001$; **E**, Comparison of proliferation rate among the HUVECs stimulated with the supernatant from normal SiHa cells (**H-SiHa-con**), the SiHa cells with Nck1 gene transfection (**H-SiHa-Nck1+**) and the SiHa cells with Nck1 siRNA (**H-SiHa-Nck1−**), *, **H-SiHa-Nck1+** vs **H-SiHa-con**, $p = 0.007$; **#**, **H-SiHa-Nck1−** vs **H-SiHa-con**, $p = 0.024$. **F**, Migration of **H-SiHa-con**. **G**, Migration of **H-SiHa-Nck1+**. **H**, Migration of **H-SiHa-Nck1−**. **I**, Comparison of the migration capacity between **H-SiHa-con**, **H-SiHa-Nck1+** and **H-SiHa-Nck1−**, *, **H-SiHa-Nck1+** vs **H-SiHa-con**, $p = 0.025$; **H-SiHa-Nck1−** vs **H-SiHa-con**, $p < 0.001$. **J**, Tube formation of **H-SiHa-con**. **K**, Tube formation of **H-SiHa-Nck1+**. **L**, Tube formation of **H-SiHa-Nck1−**. **M**, Comparison of the tube formation capacity between **H-SiHa-con**, **H-SiHa-Nck1+** and **H-SiHa-Nck1−**, *, **H-SiHa-Nck1+** vs **H-SiHa-con**, $p = 0.04$; **#**, **H-SiHa-Nck1−** vs **H-SiHa-con**, $p = 0.023$.

± 27, $p < 0.05$; 23.4 ± 7.403, $p < 0.05$,) but decreased in H-SiHa-Nck1- (77.54% ± 13.37%, $p < 0.05$; 120.33 ± 4.726, $p < 0.05$;12.2 ± 0.84, $p < 0.05$), compared to H-SiHa-con (102.50% ± 15.01%; 175 ± 5.292; 16.8 ± 2.049) respectively. These results indicate that Nck1 promotes the angiogenesis-inducing ability of SiHa cells.

3.3. Nck1 enhanced the angiogenesis-inducing capacity of CSCC via MMP2

Given that Nck1 increased the angiogenesis-inducing ability of the cancer cells, we hypothesized that angiogenic molecules may involve in this process. So, we detected VEGF and MMP2 levels in SiHa, SiHa-Nck1 + and SiHa-Nck1-. As shown, the expression level of VEGF was comparable among the three groups (Fig. 3A). However, the level of MMP2 was increased in SiHa-Nck+ (1.374 ± 0.163, $p < 0.05$) but decreased in SiHa-Nck1− (0.238 ± 0.026, $p < 0.05$), compared to SiHa cells (0.970 ± 0.176, Fig. 3A), suggesting MMP2 is down-stream of Nck1. This was further supported by ELISA analysis. Similarly, the supernatant MMP2 level was also found to be increased in SiHa-Nck1+ (951.53 ± 66.88 pg, $p < 0.05$) but decreased in SiHa-Nck1- (652.47 ± 56.96 pg, $p < 0.05$), compared to SiHa cells (757.77 ± 19.30 pg) (Fig. 3B–C). To further confirm the role of MMP2 in angiogenesis, the recombinant human MMP2 protein (ab125181, abcam, USA) was also used to stimulate HUVECs. As shown in Fig. 3D–F, the proliferation, migration and tube formation capacity of HUVECs were increased in a concentration-dependent manner. Together, these results reveal that Nck1-MMP2 mediates enhancement of the angiogenesis-inducing capacity in cervical squamous carcinoma cells.

3.4. NCK1-induced upregulation of MMP2 was mediated by RAC1-PAK1 signaling

Nck1 has been reported to activate a downstream small G protein-Rac1 which can further activate PAK1 [25]. So we next determined whether this pathway was involved in Nck1-MMP2 signaling. Intriguingly, Rac1-GTP (activated form of Rac1), p-PAK1 and MMP2 levels were up-regulated in SiHa-Nck1+ but decreased in SiHa-Nck1−, compared to control cells (Fig. 4A). Specifically, the levels were 0.209 ± 0.032 vs 0.0623 ± 0.0058, 0.571 ± 0.045 vs 0.024 ± 0.006 and 1.016 ± 0.129 vs 0.348 ± 0.072 for Rac1-GTP, p-PAK1 and MMP2 respective in SiHa-Nck1+ vs SiHa-Nck1−. These data indicate that Nck1 initiates a Rac1-GTP, p-PAK1 and MMP2 cascade signaling. We then examined how this cascade works. Firstly, Rac1 inhibitor (NSC23766) was used as Nck1 can activate Rac1 directly. As expected, Rac1 was inhibited with the inhibitor in the SiHa-Nck1+ (0.043 ± 0.022, $p < 0.05$). More interestingly, p-PAK1 (0.218 ± 0.016, $p < 0.05$) and MMP2 (0.504 ± 0.001, $p < 0.05$) levels were also decreased by this inhibitor, compared vehicle in normal SiHa-Nck1+. These results demonstrate that Rac1 is up-stream signal of PAK1and MMP2. To further investigate the sequence of PAK1 and MMP2 signaling, SiHa-Nck1+ were pre-treated with PAK1 inhibitor (IPA-3). With PAK1 signaling inhibition (0.344 ± 0.036 vs 0.851 ± 0.087, $t = 9.323$, $p < 0.05$, Fig. 4B), only MMP2 level was decreased (0.686 ± 0.153 vs 1.374 ± 0.163, $p < 0.05$), but not Rac1-GTP (5.595 ± 0.116 vs 5.535 ± 0.304, $p > 0.05$), indicating that PAK1 is up-stream of MMP2 signaling. Altogether, the cascade of Nck1-Rac1-PAK1-MMP2 signaling was unveiled.

3.5. Nck1-induced angiogenesis of CSCC is dependent on the activation of Rac1-PAK1 signaling

Since the Nck1-Rac1-PAK1-MMP2 cascade was identified, we then asked whether inhibition of Rac1 or PAK1 can also inhibit Nck1-induced angiogenesis. Supernatant from Rac1 or PAK1-inhibited SiHa-Nck1+ was also used to stimulate HUVECs (named H-Nck1+-NSC23766 and H-Nck1+-IPA-3). As expected, the proliferation (Fig. 4C), migration (Fig. 4D–G) and tabulation (Fig. 4H–K) of H-NCK1

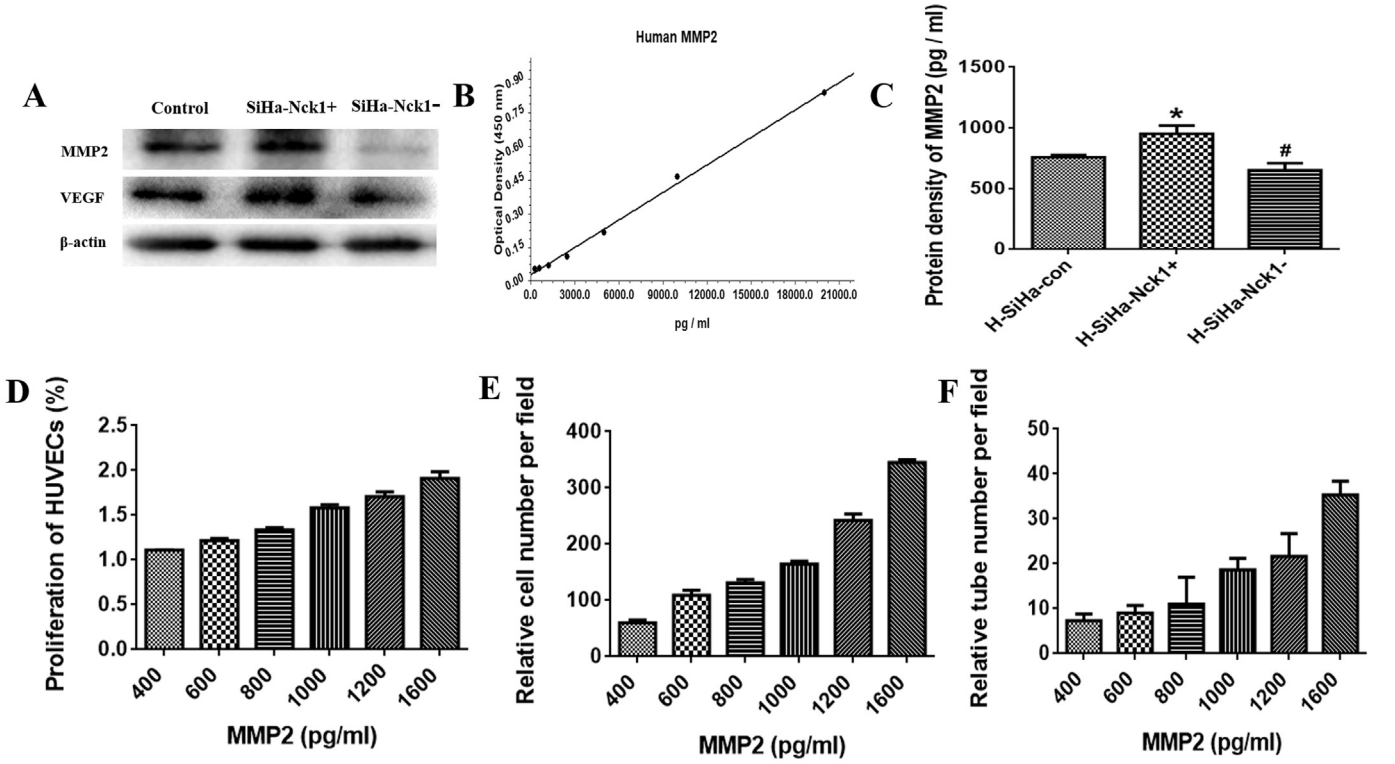

Fig. 3. The effect of Nck1 on expression of pro-angiogenic factors in SiHa cells. **A**, VEGF level was comparable between the SiHa cells (**control**), **SiHa-Nck1+** and **SiHa-Nck1−**. The **SiHa-Nck1+** and **SiHa-Nck1−** expressed a notably higher and lower level of MMP2 than SiHa cells, respectively. **SiHa-Nck1+** vs **control**, $p < 0.001$; **SiHa-Nck1−** vs **control**, $p < 0.001$. **B**, Standard curve of MMP2 ELISA. **C**, The supernatant MMP2 levels in **H-SiHa-Nck1+** and **H– SiHa-Nck-** are respectively higher and lower than that of **H-SiHa-con**. *, **H-SiHa-Nck1+** vs **H-SiHa-con**, $p = 0.03$; **#**, **H-SiHa-Nck1−** vs **H-SiHa-con**, $p = 0.039$. **D**, Proliferation of HUVECs was increased in a MMP2 concentration-dependent manner. **E**, Migration of HUVECs was increased in a MMP2 concentration-dependent manner. **F**, Tube formation of HUVECs was increased in a MMP2 concentration-dependent manner.

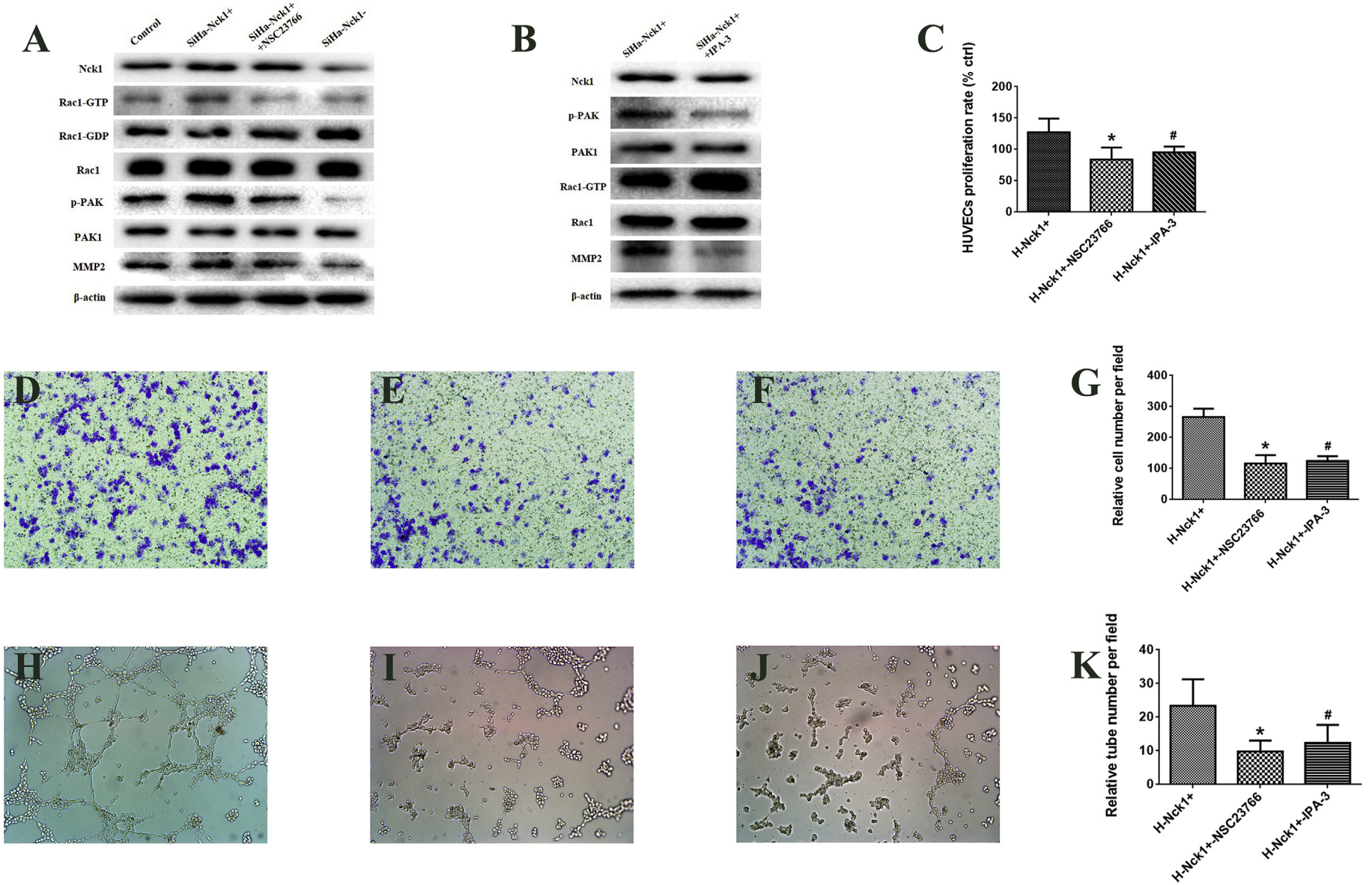

Fig. 4. The role of Rac1/PAK1 signal pathway in Nck1-medaited MMP2 up-regulation and Nck1-induced angiogenesis. **A**, The levels of Rac1-GTP, p-PAK and MMP2 were significantly higher in **SiHa-Nck1+** but lower in **SiHa-Nck1−** than that of normal SiHa cells (**Control**) (**SiHa-Nck1+** vs **Control:** $p = 0.045$, $p < 0.001$ and $p = 0.025$; **SiHa- Nck1−** vs **Control:** $p = 0.047$; $p = 0.008$; $p = 0.004$). The levels of Rac1-GTP, p-PAK1 and MMP2 in SiHa-Nck1+ with NSC23766 (**SiHa-Nck1++NSC23766**) were clearly lower than their levels in **SiHa-Nck1+** (**SiHa-Nck1++NSC23766 vs SiHa-Nck1+**, $p = 0.003$, $p = 0.002$ and $p = 0.012$). **B**, The levels of p-PAK1 and MMP2 in the SiHa-Nck1+ pre-treated with the specific inhibitor of PAK1 (**SiHa-Nck1++IPA-3**) were significantly lower than that of **SiHa-Nck1+** (**SiHa-Nck1++IPA-3 vs SiHa-Nck1+**, $p < 0.001$ and $p = 0.006$). **C**, Comparison of proliferation rate between the HUVECs stimulated with the supernatant from SiHa-Nck1+ (**H-Nck1+**), the SiHa-Nck1 + with Rac1 inhibition (**H-Nck1 + -NSC23766**) and the SiHa-Nck1+ with PAK inhibition (**H-Nck1 + −IPA-3**); *, **H-Nck1 + -NSC23766** vs **H-Nck1+**, $p = 0.01$; **#**, **H-Nck1 + -IPA-3** vs **H-Nck1+**, $p = 0.018$. **D**, Migration of **H-Nck1+**. **E**, Migration of **H-Nck1 + -NSC23766**. **F**, Migration of **H-Nck1 + -IPA-3**. **G**, Migration ability of **H-Nck1 + -NSC23766** and **H-Nck1 + -IPA-3** was significantly lower than that of **H-Nck1+**. *, **H-Nck1 + -NSC23766** vs **H-Nck1+**, $p = 0.02$; **#**, **H-Nck1 + -IPA-3** vs **H-Nck1+**, $p = 0.01$. **H**, Tube formation of **H-Nck1+**. **I**, Tube formation of **H-Nck1 + -NSC23766**. **J**, Tube formation of **H-Nck1 + -IPA-3**. **K**, The tube formation capacity of **H-Nck1 + -NSC23766** and **H-Nck1 + -IPA-3** was clearly lower than that of **H-Nck1+**. *, **H-Nck1 + -NSC23766** vs **H-Nck1+**, $p = 0.07$; **#**, **H-Nck1 + -IPA-3** vs **H-Nck1+**, $p = 0.032$.

+ -NSC23766 (83.90% ± 19.22%, $p < 0.05$; 116.667 ± 26.652, $p < 0.05$; 9.8 ± 3.27, $p < 0.05$) and H-Nck1 + -IPA-3 (95.34% ± 9.26%, $p < 0.05$; 124.667 ± 14.742, $p < 0.05$; 12.4 ± 5.32, $p < 0.05$) were both decreased, compared to H-Nck1+ (127.24% ± 22.03%; 266 ± 27.00; 23.4 ± 7.89). The results further support that Rac1 and PAK1 are crucial for Nck1 function on promoting the angiogenesis-inducing capacity of SiHa cells.

4. Discussion

Nck1 has been shown to play oncogenic roles in cancers by regulating growth and invasion of cancer cells [22–24]. Song et al. [26] reported that there was noticeable expression difference of Nck1 between cervical cancer and normal cervical epithelial tissue, implying Nck1 may implicate in the development and progression of cervical cancer. However, the association between Nck1 and cancer angiogenesis remains unclear.

Nck1 expression was found to increase in pre-invasive tissues from CIN patients and associate with grades of CIN, and the overexpression of Nck1 was determined in CSCC tissues. Moreover, Nck1 expression was related to the aggressive clinical behavior, including lymph node metastasis, parametrial involvement, vascular invasion and clinical stage. Immunohistochemistry results suggested that Nck1 may involve in the carcinogenesis and progression of CSCC, consistent with previous report [26]. With endothelial CD34 labeling, the MVD of CSCC was evaluated and the expression of Nck1 was shown to be positively correlated with the cancer MVD, indicating an association between Nck1 and angiogenesis in CSCC.

To verify the association of Nck1 with the angiogenesis of CSCC, the expression level of Nck1 in the CSCC cells was detected. We found Nck1 modulated endothelial angiogenic functions, such as proliferation, migration and tube formation. Cancer angiogenesis is generally regulated by two basic mechanisms, namely, the paracrine effect and the autocrine effect. The former is mediated by cancer cell-derived pro-angiogenic molecules, while the latter is mediated by the endothelial cell-derived factors. As Nck1 in itself is not a secretory protein, we deduced that Nck1 might regulate some downstream paracrine angiogenic factors. Thus, we further evaluated the levels of two common angiogenic factors (VEGF and MMP2) in the cancer cells with different Nck1 levels. The VEGF expression level was comparable between those cancer cells. Interestingly, MMP2 was up-regulated in the cancers cells with Nck1 gene transfection while was reduced in the cancer cells with Nck1 siRNA. To further confirm cancer cell-derived secretion of MMP2 as a downstream angiogenic effector of Nck1, we used recombinant MMP2 protein to stimulate endothelial cells and found the endothelial angiogenesis ability was increased in a MMP2 dose-dependent manner. Together, these results suggest that Nck1 promotes the angiogenesis ability of cervical squamous carcinoma cells in a MMP2-dependent paracrine pathway. Indeed, a recent study revealed the regulatory role of Nck1 on MMP14 [25], indicating other angiogenic factors may involve in this process.

As an intracellular signal adapter [29–31], Nck1 recruits and activates downstream small G proteins through SH2/SH3 domains. Nck1 has been demonstrated to regulate the activity of Rho family GTPases, typically activating Rac1 [32]. We also found the activation of Rac1 in the cancer cells with Nck1 overexpression. PAK1 is the main downstream signal of Rac1 and Rac1/PAK1 signaling has also been reported to be involved in angiogenesis [32]. Therefore, we further observed whether Rac1/PAK1 signaling also implicated in Nck1-induced angiogenesis of CSCC. In cancer cells overexpressing Nck1, Rac1 activation led to increase of p-PAK1 and MMP2 levels and Rac1 inhibition reduced their levels. Moreover, PAK1 inhibition led to reduction of MMP2 on Rac1 activation, suggesting Nck1 triggers a Rac1/PAK1 cascade to up-regulate MMP2. To further confirm the role of Rac1 and PAK1 activation in Nck1-induced angiogenesis, we also observed the effect of Rac1 and PAK1 inhibition upon the pro-angiogenic role of Nck1 in the cancer cells overexpressing Nck1. As expected, inhibition of Rac1 or PAK1 impaired Nck1-induced angiogenesis capacity in CSCC. Together, we demonstrated the Nck1/Rac1/PAK1/MMP2 cascades on angiogenesis capacity of CSCC. Interestingly, Gonzalez et al. [25] found that Rac1/Pak1/p38/MMP2 axis regulated the angiogenesis of ovarian cancer and Zhang et al. [33] described Nck1/STAT3/PAK1/ERK signaling in cancer metastasis and angiogenesis of colorectal carcinoma. However, all the studies have limitations on finding relationship between PAK1 and MMP2. PAK1 activation has been shown to involve in the progression of cancers [34–37], and has been found to be associated with poor biological behavior and prognosis of clinical cervical cancer [38]. Therefore, our results also suggest Nck1 is involved in the progression of CSCC. In addition, Nck1 may also regulate other biological process of cervical cancer cells as MMP2 has been reported to play important roles in cancer growth [39], invasion and metastasis [40]. Moreover, a recent study [41] found that a long-chain ncRNA of Nck1 gene (LncRNA NCK1-AS1) was up-regulated in cervical cancer tissues and promoted proliferation and invasion of CSCC in vitro. Therefore, Nck1 may regulate the progression of CSCC through various biological mechanisms except angiogenesis.

In summary, we identified a novel Nck1/Rac1/PAK1/MMP2 cascade that is critical for angiogenesis of CSCC. This provides evidence for novel therapeutic avenue of targeting Nck1 in CSCC.

Conflict of interest statement

The authors declare that there are no conflicts of interest.

Author contribution

1. Xia Pei was responsible for much of the molecular biological experiments, including western blotting, qPCR and endothelial cellular functional experiments, and wrote the manuscript.
2. Huang Mingchuan collected the clinic cervical squamous carcinoma samples and also made contribution to the manuscript drafting.
3. Zhang Yuting made contribution to the cell culture, gene transfection and siRNA.
4. Xiong Xiujan finished the immunohistochemistry work including the microvessel endothelial labeling.
5. Yan Min contributed to the ELISA assay and data statistical analysis.
6. Xiong Xiaoliang completed the histological identification of all the clinical samples and quantified the tumor microvessel density.
7. Yu Weiwei also made contribution to the identification of cancer samples and microvessel density assessment.
8. Song Enlin was the correspondence author who established this project, raised funds, made overall plans of experimental process and corrected the paper.

References

[1] F. Azam, S. Mehta, A.L. Harris, Mechanisms of resistance to antiangiogenesis therapy, Eur. J. Cancer 46 (8) (2010) 1323–1332.
[2] S. Ruderman, A. Eshein, V. Valuckaite, et al., Early increase in blood supply (EIBS) is associated with tumor risk in the Azoxymethane model of colon cancer, BMC Cancer 18 (1) (2018) 814.
[3] V.W.M. van Hinsbergh, P. Koolwijk, Endothelial sprouting and angiogenesis: matrix metalloproteinases in the lead, Cardiovasc. Res. 78 (2) (2008) 203–212.
[4] H. Sasaki, S. Morohashi, T. Toba, et al., Neoangiogenesis of gastric submuosa-invasive adenocarcinoma, Oncol. Lett. 16 (3) (2018) 3859–3900.
[5] H. Wang, M. Zhan, R. Yang, et al., Elevated expression of NFE2L3 predicts the poor prognosis of pancreatic cancer patients, Cell Cycle 17 (17) (2018) 2164–2174.
[6] R.N.F. Silva, L.B. Dallarmi, A.K.C. Araujo, et al., Immunohistochemical anlysis of neurtophils, interleukin-17, matrix metalloproteinase-9, and neoformed vessels in oral squamous cell carcinoma, J. Oral Pathol. Med. 47 (9) (2018) 856–863.
[7] S. Wang, Z. Xia, Z. Hong, et al., FOXF1 prootes angiogenesis and accelerates bevacizumab resistance in colorectal cancer by transcriptionally activating VEGFA, Cancer Lett. e39 (2018) 78–90, https://doi.org/10.1016/j.canlet.208.09.026 (Epb 2018 Sep 22).
[8] A.H. Rahmani, A.Y. Babiker, M.A. Alsahli, et al., Prognostic significance of vascular endothelial growth factor (VEGF) and Her-2 Protein in the genesis of cervical carcinoma, Open access Macedonian journal of medical sciences 6 (2) (2018) 263–268.
[9] M. Inokuchi, M. Nakagawa, N. Baogok, et al., Prognostic significance of high EphA1–4 expression levels in locally advanced gastric cancer, Anticancer Res. 38 (3) (2018) 1685–1693.

[10] H.S. Kim, G. Yoon, J.Y. Ryu, et al., Sphingosine kinase 1 is a reliable prognostic factor and a novel therapeutic target for uterine cervical, Oncotarget 6 (29) (2015) 26746–26756.
[11] L.J. Liang, Y.X. Wen, Xia, et al., Apatinib combined with docetaxel as a salvage treatment for metastatic esophageal squamous cancer: a case report, Onco Targets Ther. 11 (2018) 5821–5826, https://doi.org/10.2147/OTT.S174429 (eCollection 2018).
[12] Z. Yang, G. Chen, Y. Cui, et al., The safety and efficacy of TACE combined with apatinib on patients with advanced hepatocellular carcinoma: a retrospective study, Cancer Biol. Ther. 17 (2018) 1–7, https://doi.org/10.1080/15384047.2018.1529099 (Epub ahead of print).
[13] L.E. Minon, K.S. Tewari, Cervical cancer-state of the science: from angiogenesis blockade to checkpoint inhibition, Gynecol. Oncol. 148 (3) (2018) 609–621.
[14] H.C. Hsu, N. Lapke, S.J. Chen, et al., PTPRT and PTPRD deleterious mutations and deletion predict Bevacizumab resistance in metastatic colorectal cancer patients, Cancer 10 (9) (2018)https://doi.org/10.3390/cancers pii:E314. (10090314).
[15] T. Simon, S. Pinioti, P. Schellenberger, et al., Shedding of bevacizumab in tumour cells-derived extracellular vesicles as a new therapeutic escape mechanism in glioblastoma, Mol. Cancer 17 (1) (2018) 132.
[16] J.W. Moroney, M.P. Schlumbrecht, T. Helgason, et al., A phase I trial of liposomal doxorubicin, bevacizumab, and temsirolimus in patients with advanced gynecologic and breast malignancies, Clin. Cancer Res. 17 (21) (2011) 6840–6846.
[17] F. Bladt, E. Aippersbach, S. Gelkop, et al., The murine Nck SH2/SH3 adaptors are important for the development of mesoderm-derived embryonic structures and for regulating the cellular actin network, Mol. Cell. Biol. 23 (13) (2003) 4586–4597.
[18] A. Ruusala, T. Pawson, C.H. Heldin, et al., Nck adapters are involved in the formation of dorsal ruffles, cell migration, and Rho signaling downstream of the platelet-derived growth factor beta receptor, J. Biol. Chem. 283 (44) (2008) 30034–30044.
[19] Q. Zhou, T. Huang, Y.E. Wang, et al., Identification of Max binding protein as a novel binding protein of Nck1 and characterization of its role in inhibiting human liver cancer SK-HEP-1 cells, Chin. Med. J. 125 (18) (2012) 3336–3339.
[20] H. Li, B. Li, L. Larose, IRE1 alpha links Nck1 deficiency to attenuated PTP1B expression in HepG2 cells, Cell. Signal. 36 (2017) 79–90.
[21] Y. Miyamoto, T. Torii, K. Kawahara, et al., Dock8 interacts with Nck1 in mediating Schwann cell precursor migration, Biochem Biophy Rep. 6 (2016) 113–123.
[22] D.C. Morris, J.L. Popp, L.K. Tang, et al., Nck deficiency is associated with delayed breast carcinoma progression and reduced metastasis, Mol. Biol. Cell 28 (24) (2017) 3500–3516.
[23] N.W. West, A. Garcina-Vargas, C.E. Chalfant, et al., OSU-03012 sensitizes breast cancers to lapatinib-induced cell killing: a role for Nck1 but not Nck2, BMC Cancer 13 (256) (2013).
[24] G. Zhang, X. Chen, F. Qiu, et al., A novel interaction between the SH2 domain of signaling adaptor protein Nck-1 and the upstream regulator of the Rho family GTPase Rac1 engulfment and cell motility 1 (ELMO1) promotes Rac1 activation and cell motility, J. Biol. Chem. 289 (33) (2014) 23112–23122.
[25] V. Gonzalez-Villasana, E. Fuentes-Mattei, C. Ivan, et al., Rac1/Pak1/p38/MMP-2 axis regulates angiogenesis in ovarian cancer, Clin. Cancer Res. 21 (9) (2015) 2127–2137.
[26] J.Y. Song, H.S. Bae, H. Koo do, et al., Candidates for tumor markers of cervical cancer discovered by proteomic analysis, J. Korean Med. Sci. 27 (12) (2012) 1479–1485.
[27] Y. Zhang, P. Xia, W. Zhang, et al., Short interfering RNA targeting Net1 reduces the angiogenesis and tumor growth of in vivo cervical squamous cell carcinoma through VEGF down-regulation, Hum. Pathol. 65 (2017) 113–122.
[28] G. Tu, G. Li, H. Peng, et al., P2X(7) inhibition in stellate ganglia prevents the increased sympathoexcitatory reflex via sensory-sympathetic coupling induced by myocardial ischemic injury, Brain Res. Bull. 96 (2013) 71–85.
[29] M. Huang, S. Anand, E.A. Murphy, et al., EGFR-dependent pancreatic carcinoma cell metastasis through Rap1 activation, Oncogene 31 (22) (2012) 2783–2793.
[30] W. Li, P. Hu, E.Y. Skolnik, et al., The SH2 and SH3 domain-containing Nck protein is oncogenic and a common target for phosphorylation by different surface-receptors, Mol. Cell. Biol. 12 (12) (1992) 5824–5833.
[31] M.M. Chou, J.E. Fajardo, H. Hanafusa, The SH2-containing and SH3-containing Nck protein transforms mammalian fibroblasts in the absence of elevated phosphotyrosine levels, Mol. Cell. Biol. 12 (12) (1992) 5834–5842.
[32] J.L. Reinardy, D.M. Corey, C. Golzio, et al., Phosphorylation of threonine 794 on Tie1 by Rac1/PAK1 reveals a novel angiogenesis regulatory pathway, PLoS One 10 (10) (2015), e0139614. .
[33] F. Zhang, Y.X. Lu, Q. Chen, et al., Identification of NCK1 as a novel downstream effector of STAT3 in colorectal cancer metastasis and angiogenesis, Cell. Signal. 36 (2017) 67–78.
[34] C.K. Rane, A. Minden, P21 activated kinase signaling in cancer, Semin. Cancer Biol. (2018)https://doi.org/10.1016/j.semcancer pii: S1044-579X(17)30249-3. (Epub ahead of print).
[35] F.A. Liu, Z. Cheng, X. Li, et al., A novel Pak1/ATF2/miR-132 signaling axis is involved in the hematogenous metastasis of gastric cancer cells, Mol. Ther.–Nucleic Acids 8 (2017) 370–382.
[36] S. Jiang, W.Y. Tian, Y. Yan, et al., Expression and clinical significance of MIIP and PAK1 in endometrial carcinoma, Zhonghua Zhong Liu Za Zhi 40 (5) (2018) 359–364.
[37] C. Li, H. Liu, B. Zhang, et al., Whole-exome sequencing identifies key mutated genes in T790M wildtype/cMET-unamplified lung adenocarcinoma with acquired resistance to first-generation EGFR tyrosine kinase inhibitors, J. Cancer Res. Clin. Oncol. 144 (6) (2018) 1079–1086.
[38] Y. Feng, S. Fang, M. Li, Expression of P21-activated kinase 1 and cell division control protein 42 homolog correlates with clinicopathological features and prognosis in cervical carcinoma, J. Obstet. Gynaecol. Res. 42 (7) (2016) 860–869.
[39] H. Li, Y. Zhang, J. Hai, et al., Knockdown of TRIM31 suppresses proliferation and invasion of gallbladder cancer cells by down-regulating MMP2/9 through the PI3K/Akt signaling pathway, Biomed. Pharmacother. 103 (2018) 1272–1278.
[40] J. Choi, K. Choi, E.N. Benveniste, et al., Bcl-2 promotes invasion and lung metastasis by inducing matrix metalloproteinase-2, Cancer Res. 65 (13) (2005) 5554–5560.
[41] H.Y. Li, Y. Jia, J. Cheng, et al., LncRNA NCK1-AS1 promotes proliferation and induces cell cycle progression by crosstalk NCK1-AS1/miR-6857/CDK1 pathway, Cell Death Dis. 9 (2) (2018) 198.